Linear and nonlinear transport in a small charge-tunable open quantum ring

F. G. G. Hernandez* and G. M. Gusev
Instituto de Física, Universidade de São Paulo, Caixa Postal 66318-CEP 05315-970, São Paulo, São Paulo, Brazil

Z. D. Kvon
Institute of Semiconductor Physics, Novosibirsk RU-630090, Russia

J. C. Portal
LNCMI-CNRS, UPR 3228, Boîte Postale 166, F-38042 Grenoble Cedex 9, France, INSA Toulouse, F-31077 Toulouse Cedex 4, France, and Institut Universitaire de France, F-75005 Paris, France
(Received 18 April 2011; published 16 August 2011)

We experimentally study the Aharonov-Bohm-conductance oscillations under external gate voltage in a semiconductor quantum ring with a radius of 80 nm. We find that, in the linear regime, the resistance-oscillation plot in the voltage-magnetic-field plane corresponds to the quantum ring energy spectra. The chessboard pattern assembled by resistance diamonds, while loading the ring, is attributed to a short electron lifetime in the open configuration, which agrees with calculations within the single-particle model. Remarkably, the application of a small dc current allows observing strong deviations in the oscillation plot from this pattern accompanied by a magnetic-field symmetry break. We relate such behavior to the higher-order-conductance coefficients determined by electron-electron interactions in the nonlinear regime.

DOI: 10.1103/PhysRevB.84.075332 PACS number(s): 73.23.−b

I. INTRODUCTION

In solid-state systems, quantum rings have attracted much attention for a long time because they provide a unique opportunity for the study of electron interference in the simplest form.[1–5] For electrons traveling along different ring arms, the waves acquire a phase shift due to the Aharonov-Bohm (AB) effect. The phase difference is given by $2\pi(\phi/\phi_0)$ where $\phi = \pi r_0^2 B$ is the magnetic flux enclosed by the ring with a radius r_0 in the presence of magnetic field B, and ϕ_0 is the flux quantum. This phenomenon appears in transport measurements as a modulation with period $\pi r_0^2/(h/e)$ in B when passing a current through the ring connected to multiple leads. Also, it is possible to realize additional tuning of electron interference in the ring by gate voltage[3,6,7] and dc bias.[8]

For a ring interferometer, the Casimir-Onsager relation implies that the AB-oscillation phase must remain rigid to obey symmetry rules in the magnetic field, so it can only change in π jumps.[6,9,10] While this relation does not hold out of equilibrium, it has been predicted to be an asymmetric component for mesoscopic conductors in different configurations.[11–13] This question has been addressed for several systems, such as rings,[14,15] quantum dots,[16,17] and carbon nanotubes.[18]

In a quantum ring, AB oscillations can be mapped onto the details of the confining potential and on the related energy-shell-structure properties.[6,19] The possibility to extend the single-electron modeling for many-electron semiconductor rings has been demonstrated experimentally.[20] The energy spectra for closed quantum rings were measured by magnetotransport in the rings containing about 200 electrons (two to three radial sub-bands).[20] Also, the energy spectra were determined by optical spectroscopy in self-assembled rings.[21,22]

Despite the above referred to demonstrations, important questions about the electronic transport properties in the few-particle loading limit remain. Here, we study the AB-conductance oscillations in a small ring with populated one to two radial sub-bands. By tuning a top voltage gate, we map the ring energy spectra in linear- and nonlinear-transport regimes. In contrast to the linear regime where the AB-oscillation plot in the voltage-magnetic-field plane shows a striking similarity to the energy spectra, we observed a strong difference between the mapped and the single-particle-modeled diagram for nonlinear-conductance oscillations.

II. EXPERIMENTAL RESULTS

The ring two-terminal interferometer that was investigated was fabricated using an AlGaAs/GaAs heterostructure with a shallow (25 nm below the sample surface) layer of a two-dimensional electron gas (2DEG) confined at the heterointerface. The electrons are supplied by a Si-doped plane located at 7.5 nm from the heterointerface. The electron mobility in the initial heterostructure was $\mu = 10^5$ cm^2 V^{-1} s^{-1} at $T = 4.2$ K, and the density was $n_s = 5 \times 10^{11}$ cm^{-2}, which corresponded to the electron mean-free path $l = 1.2$ μm. The AB ring was fabricated in the center of the Hall bar structure by means of a high-resolution electron-beam lithography followed by a fast plasma etching as described in a previous paper.[23]

The effective ring radius $r_0 = 80$ nm was determined from the AB-oscillation period. It is one of the smallest rings reported, being two times smaller than the ring used in Ref. 14 and nine times smaller than the ring used in Ref. 24. Larger rings restrict the practical magnetic-field strength due to the larger AB-oscillation frequency. A small ring radius also allows for studying the energy spectra in the few-electron regime. With a conducting region width of 20–30 nm, we estimate about 20–40 electrons in the ring.[25]

The ring was connected to the regions in the Hall bar with a 2DEG by two point contacts, and the measurements that were

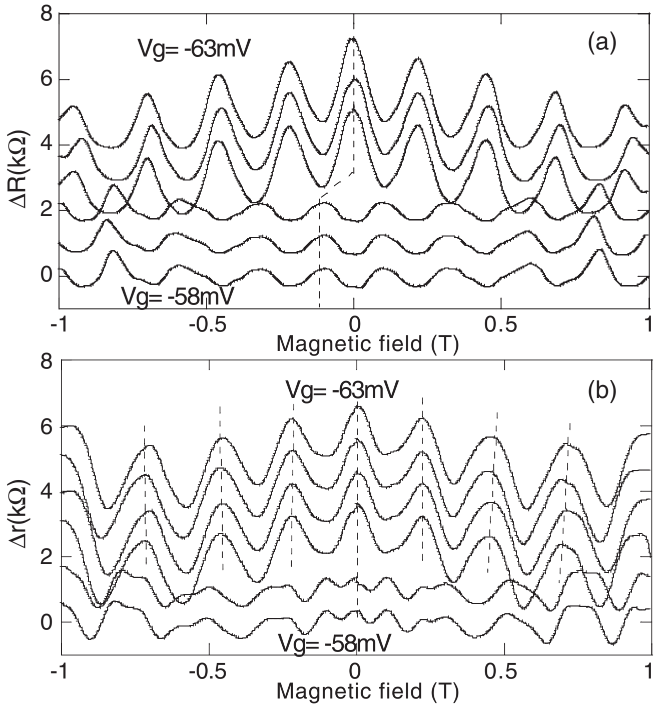

FIG. 1. AB oscillations in the magnetoresistance as a function of the gate bias V_g (5-mV windows) for (a) without I_{dc} and (b) with $I_{dc} = 500$ nA. Dashed lines are a guide to the eyes for the phase evolution.

performed were effectively two terminal. The structure was entirely covered by an Au/Ti gate. The longitudinal resistance was measured using an ac current of 1 nA at a frequency of 6.1 Hz in a four-probe Hall bar setup. Measurements have been performed in magnetic fields ranging from -1 T to 1 T and at a temperature of 50 mK. For the nonlinear-transport measurement, direct electric current $I_{dc} = 500$ nA was applied simultaneously with ac excitation through the same current leads.

The differential resistance $r = dV/dI$ has been measured as a function of the perpendicular magnetic field B for different values of the gate-voltage bias V_g. V_g produces the charge-density depletion from the gate region and allows the ring Fermi energy tuning. From the structure's geometrical capacitance, we estimate a lever arm of 2 electrons/5 mV. We used an experimental V_g step of 1 mV.

Figure 1 shows the ring resistance data in the linear and nonlinear regimes measured as a function of the magnetic field at different gate biases where the background resistance was extracted. Without I_{dc}, we found an AB maximum amplitude of 2 kΩ with the total resistance close to the value of $h/2e^2 = 12$ kΩ. Traces with the AB-oscillation average periods close to 0.2 T indicate an 80-nm ring radius. As mentioned above, the strong magnetic-symmetry constraint related to the Onsager relation allows only AB phase changes in π jumps. Thus, the AB oscillations remain rigid to keep the maximum or minimum oscillation centered at a zero magnetic field as observed in Fig. 1(a). Furthermore, we remarkably observe that the AB amplitude remains unaffected while the phase holds at a given value.

Figure 1(b) shows the AB-resistance oscillations after applying $I_{dc} = 500$ nA to the ring. The oscillation amplitude has a maximum of 2 kΩ as for AB oscillations without I_{dc}. However, significant changes are observed in the AB phase relation with the magnetic field. For the AB phase, the maxima and minima positions, at a given field, are continuously shifted and are controlled as a function of V_g with the slope depending on the field direction.

Figure 2 shows the measured data in the linear regime without I_{dc} for the gate-bias sweeping of the ring's electron density. We can observe a typical π phase jump at a zero field at $V_g = -60$ mV (blue to red in the contour plot). While increasing V_g, the resistance exhibits a chessboard pattern where the low-resistance squares enclose high-resistance squares as indicated by the diamond-shaped solid lines. Furthermore, this rigidity holds for higher fields because the phase and frequency are locked. For -40 mV $\leqslant V_g \leqslant -50$ mV, the AB amplitude is lower, but the frequency increases to $h/2e$. For $V_g \sim -35$ mV, the AB-resistance modulation amplitude is partially recovered. A similar, however, not complete, picture has to be observed in Ref. 15. Due to the small ring size, it is expected that the observed chessboard pattern corresponds to the quantized energy in the ring rather than to Thouless energy, which is the typical energy in the larger rings.[6] Therefore,

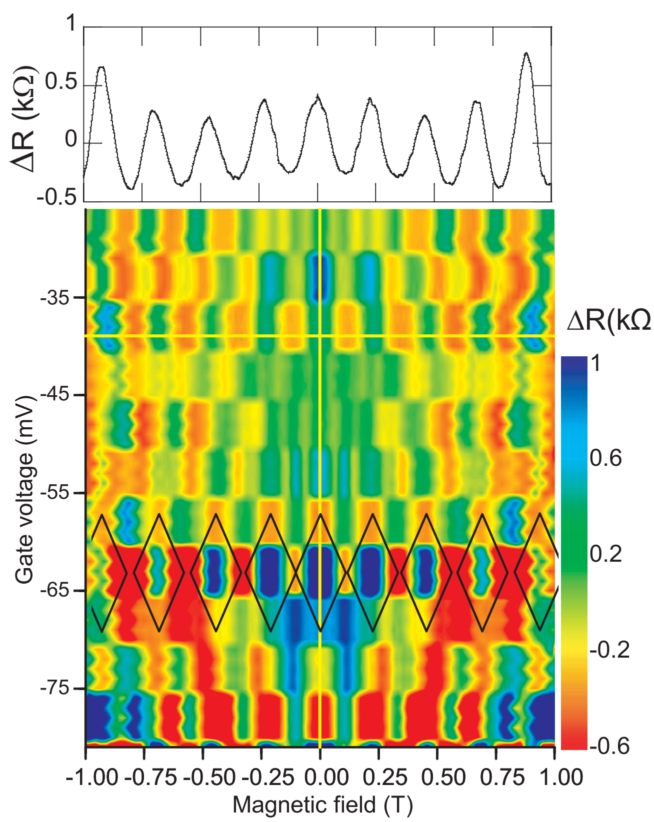

FIG. 2. (Color online) Contour plot of AB oscillations as a function of the magnetic field and gate bias at 50 mK in the absence of I_{dc} (linear regime). The experimental voltage step is 1 mV. The solid lines indicate the diamond-shaped region formed by low-resistance areas enclosing high-resistance squares in a chessboard pattern. The top panel shows the resistance at the cut indicated by the horizontal yellow line. The vertical yellow line is a guide for the zero-magnetic-field phase evolution.

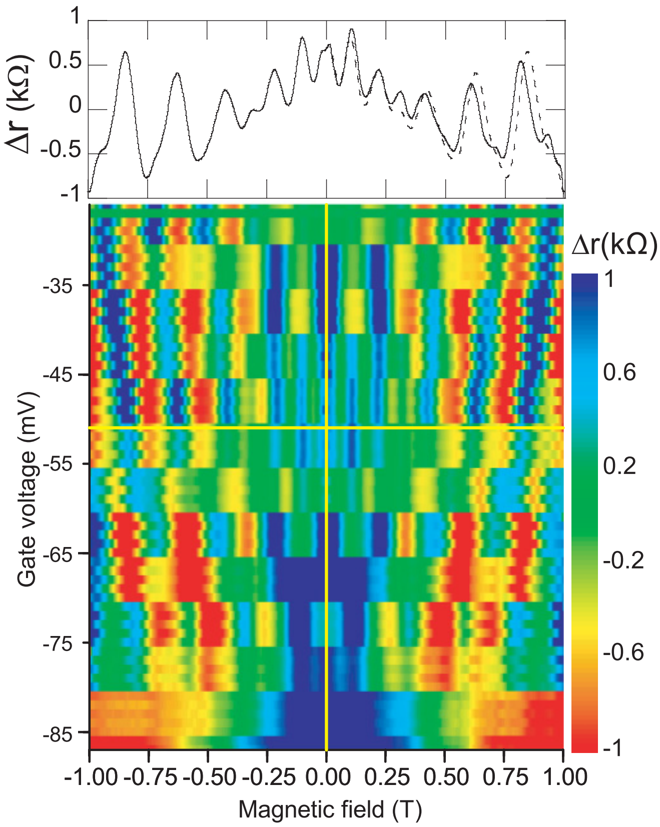

FIG. 3. (Color online) Contour plot of AB oscillations as a function of the magnetic field and gate bias at 50 mK with $I_{dc} =$ 500 nA. The experimental voltage step is 1 mV. The top panel shows the resistance at the cut indicated by the horizontal yellow line. The dashed line in the top panel displays $\Delta r(-B)$ reflected in the positive-field axis as an example of the magnetic-field asymmetry. The vertical yellow line is a guide for the zero-magnetic-field phase evolution.

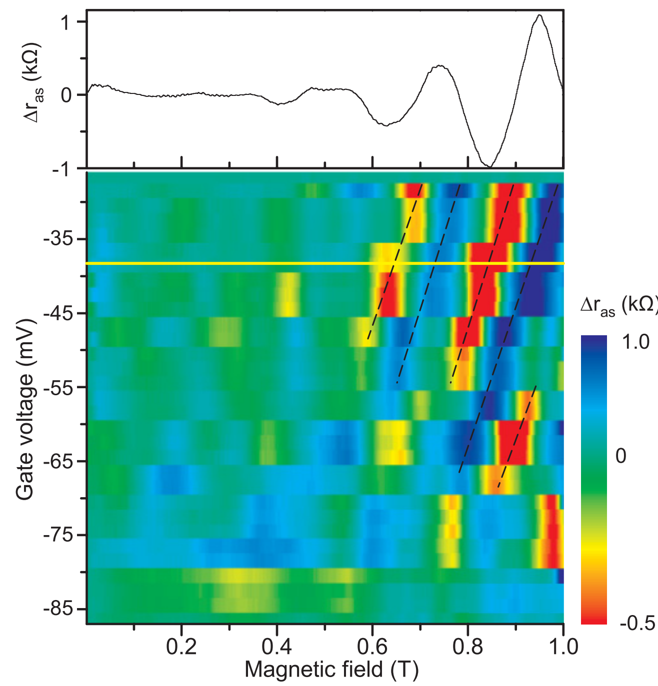

FIG. 4. (Color online) Experimental asymmetry in the differential resistance r as a function of the magnetic field. Top panel, asymmetric part of the conductance Δr_{as} at the horizontal cut indicated by the horizontal yellow line. Color scale is logarithmic.

the scale defined by π phase jumps (chessboard square size) is related to the incremental occupation of each ring level with two electrons. In the next section, we discuss the energy spectrum of the quantum ring.

In the nonlinear regime, deviations from the single-mode model are found as shown in Fig. 3. The AB oscillations in the resistance reveal the shift in the peak position with the slope depending on the magnetic-field direction. At zero magnetic field, the high-resistance regions (blue) do not evolve into low-resistance regions through the π jumps in a large range of V_g. For larger rings, the influence of the dc current, using much less current, was studied in Ref. 8.

The deviation from the chessboard pattern in the nonlinear regime is accompanied by a violation of the magnetic-field symmetry, which can be seen from the traces in Fig. 3 (top panel). The violation of the Casimir-Onsager relations in the presence of the magnetic field in the nonlinear regime has been predicted for a variety of mesoscopic systems[11–13] and has been tested experimentally in our previous paper.[15] However, a careful examination of the gate-voltage-magnetic-field dependence had not been performed. Application of a dc current would be important to establish the physics of the quantum ring, and it may exhibit other interesting phenomena. In Fig. 4, for better visualization of magnetic-field asymmetry, we display the asymmetric part of the differential resistance $\Delta r_{as} = \Delta r(-B) - \Delta r(B)$. From a comparison between Figs. 3 and 4, one may see that the phase (periodicity) change in the AB oscillations in this nonlinear regime is accompanied by a linear Δr_{as} evolution in the charge-density-magnetic-field plane. Therefore, here, we may conclude that deviations in the oscillation behavior from the single-electron model and the violation of the magnetic-field symmetry in the nonlinear regime very likely have the same physical origin.

III. DISCUSSION

In the following section, we will concentrate on the electronic properties of the quantum ring. Even when the energy spectra of the ring were discussed in early papers, we considered the single-particle model of the ring, with specific device parameters, to make our paper consistent. As mentioned above, the AB-conductance oscillations can be obtained in terms of the energy spectra. For a one-dimensional ring, the energy levels are as follows:

$$E_{l,m} = \hbar^2/2\mu r_0^2(l - m)^2, \quad (1)$$

where μ is the electron effective mass, m is the quantum number associated with the angular momentum, and $l = \phi/\phi_0$ is the number of flux quanta piercing the ring. Thus, the energy levels are parabolas with minima at $m = l$, which can be moved when increasing the magnetic field.

Figure 5(a) shows the energy levels as a function of the magnetic flux. At a given electron density, the single-particle energy oscillates in a zig-zag pattern (blue solid line) as different angular momentum states contribute to the charge

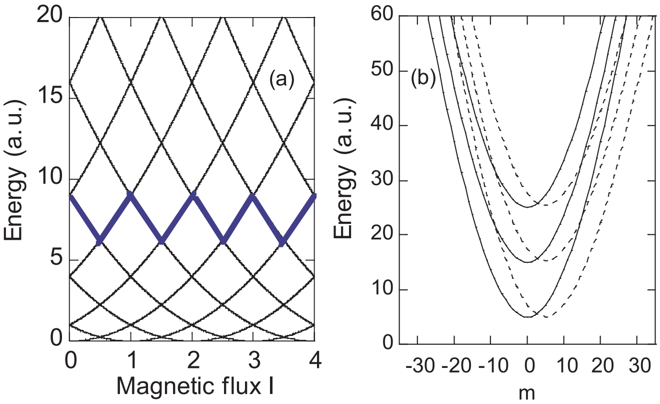

FIG. 5. (Color online) (a) Energy levels as a function of the flux for the one-dimensional ring. (b) For a bidimensional ring with many electrons, energy levels as a function of m are shown for the first three radial sub-bands at 0 T (solid line) and 1 T (dashed line).

conduction when increasing the applied field strength. Also, we can observe that there is a diamond-shaped energy gap between the filling of successive levels at a fixed flux. For the diamond-shaped gap, the top and bottom corners are connected by the loading of four electrons.

An energy-spectra model, including multiple sub-bands, may be necessary when considering the shell loading of a large number of electrons. By preserving a perfect annular symmetry but considering the ring's finite width, an analytical solution was developed for the energy spectra with radial sub-bands.[19] In this model, the ring potential is defined by

$$V(r) = a_1 r^{-2} + a_2 r^2 - V_0, \tag{2}$$

where $V_0 = 2\sqrt{a_1 a_2}$ and the constants depend on the average radius of the ring by $r_0 = (a_1/a_2)$. Near r_0, the potential takes a parabolic form with $\omega_0 = \sqrt{8a_2/\mu}$. The ring's effective width, at given Fermi energy E_F, is determined by $\Delta r = \sqrt{8E_F/\mu\omega_0^2}$. In the presence of a uniform magnetic field, the energy levels are given by

$$E_{n,m} = \left(n + \frac{1}{2} + \frac{M}{2}\right)\hbar\omega - \frac{m}{2}\hbar\omega_c - \frac{\mu}{4}\omega_0^2 r_0^2, \tag{3}$$

where n is the radial quantum number indexing the sub-band, $M = \sqrt{m^2 + 2a_1\mu/\hbar^2}$, $\omega = (\omega_c^2 + \omega_0^2)^{1/2}$, and $\omega_c = eB/\mu$.

The energy levels of the ring, as a function of the quantum number m for the first three radial sub-bands ($n = 0,1,2$), are shown in Fig. 5(b). At a given magnetic field, the sub-band minimum is given by $m_0 = eBr_0^2/2\hbar$, which is equal to the number of quantum flux l enclosed by the ring radius r_0, and again, $m = l$ determines the AB frequency as expected.

With the ring coupled to the leads, the Landauer-Büttiker formula[19,26] allows for the calculation of the ring resistance ($R = G^{-1}$) from the conductance,

$$G(B) = \frac{2e^2}{h}\sum_n T_n(B, E_F), \tag{4}$$

where T is the transmission coefficient for the nth channel in the leads that depend on the E_F position with respect to $E_{n,m}$.

Figure 6(a) shows the calculated resistance using Eq. (4) for a ring filled to the bottom of the second radial sub-band. For the

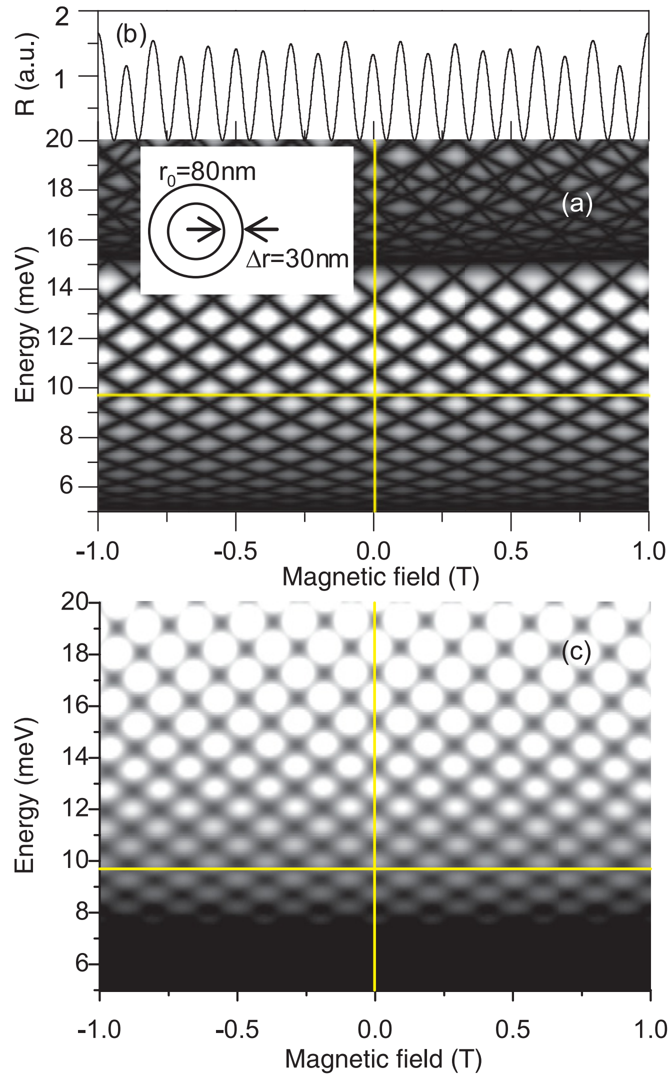

FIG. 6. (Color online) Calculated resistance as a function of the magnetic field for a ring with radius $r_0 = 80$ nm and effective width $\Delta r = 30$ nm at $E_F = 10$ meV. The bright areas have a higher resistance than the dark areas. (a) Closed ring, calculated resistance considering a long electron lifetime by including a Lorentzian broadening of 0.005 meV for the energy levels as adapted from Ref. 19. (b) Resistance with period $h/2e$ at the horizontal cut in (a). (c) Open ring, calculated resistance including a Lorentzian broadening of 1 meV for the energy levels considering a short electron lifetime.

transmission-coefficient evaluation, the m quantum number range for each n radial quantum number can be obtained from Fig. 5(b) at a given E_F and B. Also, the thermal broadening parameters were adopted from Ref. 19 as for a closed ring ($\Gamma = 0.005$ meV), and, for the effective mass, we take $\mu = 0.067m_e$. As a general feature, the Onsager magnetic-field symmetry relation is found in the overall ideal spectrum.

For the multimode spectrum, the loading of a large number of electrons in the higher radial sub-bands produces a complex picture [$E_F > 15$ meV in Fig. 6(a)]. The modification of the effective radius due to the ring's finite width is a determining factor for the observation of several AB frequencies as previously reported.[6,19] In our ring, the available number of electrons can be accommodated in the first sub-band, and the measured AB oscillations only reproduce single-mode features. Thus, we will focus our discussion below using $E_F = 15$ meV where the calculated single-mode resistance displays low-resistance lines in diamond shapes around a high-resistance core for the closed ring. The high-resistance area can be traced to the diamond-shaped energy gap obtained in Fig. 5(a), and, therefore, the AB oscillations in the magnetoresistance reflect the details of the energy spectra. Furthermore, an AB 2π phase jump indicates the filling of successive energy levels.

In the experiment (Fig. 2), we can identify the diamond-shaped regions described above. However, two main departures from the Fig. 6(a) model arise: (i): The diamond-shaped structure changes depending on the Fermi level and field with the appearance of an AB higher frequency and lower amplitude, (ii) the resistance diamonds are formed by square blocks in their apex within a chessboard pattern. For the first observation, a symmetry-breaking potential may be responsible. As demonstrated by Fig. 6(b), AB oscillations with double frequency and lower amplitude can be obtained when the Fermi energy lies between two diamond-shaped neighbors in B. Thus, the first deviation from the ideal ring can be related to weak magnetic-field-dependent states that cross the strong oscillating energy levels. It has been previously discussed that such perturbed states can be produced by a symmetry-breaking potential leading to mixed states of positive and negative angular momenta.[20]

On the other hand, by introducing a short electron lifetime for an open ring, considering an energy level broadening with a Lorentzian profile of $\Gamma = 1$ meV, the resistance calculation reproduces the square blocks in the chessboard pattern [see Fig. 6(c)]. From the measured data in Fig. 2, we obtain a chessboard-square-size scale of 5 mV in excellent agreement with the structure lever arm of 2 electrons/5 mV estimated from the geometrical capacitance. Thus, we can establish a correlation between the measured resistance pattern and the charging events in the energy spectra of the open quantum ring. In quasiballistic larger rings, the energy scale, given by a 2π AB phase change linking successive low-resistance squares (diamond-shaped top and low corners), can be determined by the Thouless energy.[6]

In the nonlinear regime (Fig. 3), further deviations from the single-particle model are observed: (i) lack of phase jumps while loading electrons at zero magnetic field, (ii) linear phase (period) evolution depending on the magnetic-field direction, (iii) magnetic-field asymmetry of the AB-oscillation amplitude. These features are fundamentally different from the observations reported in Refs. 27 and 28. In our case, the electrostatic control of the AB phase always presents a reflection in the same shift for both magnetic-field directions, while the cited reports break the phase rigidity in a multiterminal arrangement. Furthermore, we note the similarity between the behavior of the differential resistance (Fig. 3) and Δr_{as} (Fig. 4) in the nonlinear regime. It has been shown that the quadratic voltage response $G^{(2)} = I/V^2$ is represented by even and odd functions with respect to the magnetic field in the presence of the electron-electron interaction.[11–13] In diffusive mesoscopic conductors, it is expected that the odd contribution to $G^{(2)}$ exhibits random fluctuations with the magnetic field.[13] We analyzed fluctuations in the AB amplitude in our previous paper and deduced the value of the electron-electron interaction constant.

Very recently, the nonlinear conductance in a ballistic AB ring has been investigated within contact interaction approximation.[11] It has been shown that the phase rigidity in the two-terminal ring is broken by the $G^{(2)}$ conductance coefficient due to electronic interaction. This ability of phase tuning in a controlled way permits using an AB ring in the nonlinear-transport regime for interferometer study. As an example model, Ref. 11 predicts that the local variation in the electronic density in one arm of the ring gradually changes the phase of the AB oscillations in $G^{(2)}$. Examination of Fig. 4 reveals almost linear evolution for the phase shift in the AB oscillations in Δr_{as}. We obtain a slope of the phase shift of $\pi/8$ electrons. Therefore, we suggest that the deviation in the AB oscillations from single-particle behavior is attributed to the nonlinear-conductance coefficient. Note, however, that our ring is entirely covered by a metallic gate, and we are not able to separately control the local density in the arms. We explain the possible accumulated phase in the one arm by structure inhomogeneity. The origin of this inhomogeneity could be fluctuations in the arm width or potentials of the contacts connecting the leads to the ring. Calculation of the potential profile in a small ring demonstrates that the electrostatic potential is strongly asymmetric.[25] Application of the gate to the entire ring results in additional accumulation of the phase of the electrons flowing through this arm by $\Delta k L/2$, where k is the wave vector and L is the perimeter of the ring due to such potential asymmetry. In accordance with the Ref. 11 model, the electronic interaction breaks the phase rigidity for nonlinear conductance, and the AB oscillations are shifted gradually in the charge-density-magnetic-field plane. It is worth noting that, despite the possibility of breaking phase rigidity in the nonlinear regime, the monotonic behavior of the phase with B and the density is not generic and depends on model parameters, such as the screening effect of the specific device. More experimental work and theoretical effort should be performed in order to completely understand the nonlinear effects in ballistic quantum rings.

Provided that the small size of our ring with AB oscillations in the conductance has an amplitude comparable to e^2/h, there should be a large value for the nonlinear contribution $G^{(2)} \sim (\frac{e^2}{h})(\frac{e}{E_T})$ in which E_T is the Thouless energy. This observation agrees with the experimental result of the nonlinear effect from the direct-resistance-measurement method in previous studies.[14,24] For a small open quantum ring, the phase control in nonlinear transport demonstrates the possibility of using this device as a two-terminal interferometer in contrast to the phase-rigidity constraint in the linear regime.

IV. CONCLUSION

In conclusion, we have observed and have investigated AB oscillations in a semiconductor small ring in the linear and nonlinear regimes as a function of the top gate voltage. Numerous scans were taken at various V_g and magnetic-field sweeps, which allowed producing plots in the charge-density-field plane. In the linear regime, a clearly visible chessboard pattern has been obtained. We demonstrate similarity between experimental and calculated plots for an open quantum ring. The vertical chessboard scale corresponds to the occupation of each ring level with two electrons. We emphasize that the results presented here for the AB oscillations in small rings are complementary to those reported earlier for larger rings. In a previous paper, 2π phase jumps were mostly related to the shift in the Fermi level by the Thouless energy.[6] In the present case, we are probing the quantum ring spectra, and we observe a much more detailed evolution of these spectra with density.

In the nonlinear regime, we found strong deviations in the experimental plot with a chessboard pattern. Detailed examination of these results confirmed that such deviations are very likely related to the nonlinear-conductance coefficient determined by the effective electron-electron interaction parameter. Comparison with a recent theoretical study on the nonlinear transport in a ballistic quantum ring[11] agrees with our observation, if we include the sample asymmetry in the model. Due to the small size of our device and the large amplitude of the AB oscillations, the nonlinear-conductance coefficient is comparable with the linear contribution, and we are able to detect the violation of the phase rigidity directly in conductance measurements. The gradual phase shift in the AB oscillations in the nonlinear conductance provides further confirmation of the importance of the electron interaction in mesoscopic devices and may help in designing future two-terminal interferometers.

ACKNOWLEDGMENTS

Financial support for this work by the FAPESP, the CNPq (Brazilian agencies), the USP-COFECUB (Grant No. Uc Ph 109/08), the FAPESP-CNRS, the RFBI (Grant No. 11-02-00982-a), and the RAS programs for the fundamental research in nanotechnology and nanomaterials and condensed-matter quantum physics is acknowledged.

*felixggh@if.usp.br

[1]S. Washburn and R. A. Webb, Rep. Prog. Phys. **55**, 1311 (1992).
[2]G. Timp, A. M. Chang, J. E. Cunningham, T. Y. Chang, P. Mankiewich, R. Behringer, and R. E. Howard, Phys. Rev. Lett. **58**, 2814 (1987).
[3]C. J. B. Ford, T. J. Thornton, R. Newbury, M. Pepper, H. Ahmed, D. C. Peacock, D. A. Ritchie, J. E. F. Frost, and G. A. C. Jones, Appl. Phys. Lett. **54**, 22 (1989).
[4]A. A. Bykov, Z. D. Kvon, E. B. Olshanetsky, L. V. Litvin, Yu. V. Nastaushev, V. G. Mansurov, V. P. Migal, S. P. Moshchenko, and V. G. Plyukhin, JETP Lett. **57**, 613 (1993).
[5]M. Cassé, Z. D. Kvon, G. M. Gusev, E. B. Olshanetskii, L. V. Litvin, A. V. Plotnikov, D. K. Maude, and J. C. Portal, Phys. Rev. B **62**, 2624 (2000).
[6]E. B. Olshanetskii, M. Casse, Z. D. Kvon, G. M. Gusev, L. V. Litvin, A. V. Plotnikov, D. K. Maude, and J. C. Portal, Physica E **6**, 322 (2000).
[7]S. Pedersen, A. E. Hansen, A. Kristensen, C. B. Sorensen, and P. E. Lindelof, Phys. Rev. B **61**, 5457 (2000).
[8]M. Casse, E. B. Olshanetsky, Z. D. Kvon, D. K. Maude, and J. C. Portal, Physica E **7**, 781 (2000).
[9]Y. Gefen, Y. Imry, and M. Y. Azbel, Phys. Rev. Lett. **52**, 129 (1984).
[10]A. Yacoby, M. Heiblum, D. Mahalu, and H. Shtrikman, Phys. Rev. Lett. **74**, 4047 (1995).
[11]A. R. Hernández and C. H. Lewenkopf, Phys. Rev. Lett. **103**, 166801 (2009).
[12]D. Sánchez and M. Büttiker, Phys. Rev. Lett. **93**, 106802 (2004); Phys. Rev. B **72**, 201308(R) (2005).
[13]B. Spivak and A. Zyuzin, Phys. Rev. Lett. **93**, 226801 (2004); E. Deyo, B. Spivak, and A. Zyuzin, Phys. Rev. B **74**, 104205 (2006).
[14]R. Leturcq, D. Sánchez, G. Götz, T. Ihn, K. Ensslin, D. C. Driscoll, and A. C. Gossard, Phys. Rev. Lett. **96**, 126801 (2006).
[15]G. M. Gusev, Z. D. Kvon, E. B. Olshanetsky, and A. V. Plotnikov, Europhys. Lett. **88**, 47007 (2009).
[16]D. M. Zumbühl, C. M. Marcus, M. P. Hanson, and A. C. Gossard, Phys. Rev. Lett. **96**, 206802 (2006).
[17]C. A. Marlow, R. P. Taylor, M. Fairbanks, I. Shorubalko, and H. Linke, Phys. Rev. Lett. **96**, 116801 (2006).
[18]J. Wei, M. Shimogawa, Z. Wang, I. Radu, R. Dormaier, and D. H. Cobden, Phys. Rev. Lett. **95**, 256601 (2005).
[19]W.-C. Tan and J. C. Inkson, Phys. Rev. B **53**, 6947 (1996); Semicond. Sci. Technol. **11**, 1635 (1996).
[20]A. Fuhrer, S. Lüscher, T. Ihn, T. Heinzel, K. Ensslin, W. Wegscheider, and M. Bichler, Nature (London) **413**, 822 (2001).
[21]A. Lorke, R. J. Luyken, A. O. Govorov, J. P. Kotthaus, J. M. Garcia, and P. M. Petroff, Phys. Rev. Lett. **84**, 2223 (2000).
[22]R. J. Warburton, C. Schäflein, D. Haft, F. Bickel, A. Lorke, K. Karrai, J. M. Garcia, W. Schoenfeld, and P. M. Petroff, Nature (London) **405**, 926 (2000).
[23]Z. D. Kvon, D. A. Kozlov, E. B. Olshanetsky, A. E. Plotnikov, A. V. Latyshev, and J. C. Portal, Solid State Commun. **147**, 230 (2008).
[24]L. Angers, E. Zakka-Bajjani, R. Deblock, S. Guéron, H. Bouchiat, A. Cavanna, U. Gennser, and M. Polianski, Phys. Rev. B **75**, 115309 (2007).
[25]V. A. Tkachenko, Z. D. Kvon, D. V. Sheglov, A. V. Latyshev, A. I. Toropov, O. A. Tkachenko, D. G. Baksheyev, and A. L. Aseev, JETP Lett. **79**, 136 (2004).
[26]M. Büttiker, Y. Imry, R. Landauer, and S. Pinhas, Phys. Rev. B **31**, 6207 (1985).
[27]S. S. Buchholz, S. F. Fischer, U. Kunze, M. Bell, D. Reuter, and A. D. Wieck, Phys. Rev. B **82**, 045432 (2010).
[28]C. Kreisbeck, T. Kramer, S. S. Buchholz, S. F. Fischer, U. Kunze, D. Reuter, and A. D. Wieck, Phys. Rev. B **82**, 165329 (2010).